JOURNAL OF MATERIALS SCIENCE 33 (1998) 347–355

Effects of pre-existent crack in double and gradient coatings on the crack extension into fibre and interfacial debonding

S. OCHIAI, M. HOJO
Mesoscopic Materials Research Center, Faculty of Engineering, Kyoto University, Sakyo-ku, Kyoto 606-01, Japan

When a crack is formed on a fibre surface by the premature fracture of the coating, crack extension into the fibre or interfacial debonding between fibre and coating occurs, affecting the strength of the coated fibre. In the present work, the influence of pre-existent crack in double and gradient coating layers on the crack extension and interfacial debonding was studied to find the condition to improve the strength of the coated fibre. It is shown that, in both types of coating, (i) the energy release rates for crack extension into the fibre and for interfacial debonding become low when the inner coating portion adjacent to the fibre has low Young's modulus, while they become high when the inner portion has a high Young's modulus, and (ii) the ratio of the energy release rate for debonding to that for crack extension into the fibre is approximately 0.3. These results suggest that the reduced fibre strength by crack extension into the fibre in the case of strong interfacial bonding can be raised by double and gradient coatings with reduced Young's modulus of the inner coating portion. Alternatively it can be increased by weakening the interface so that the critical energy release rate for debonding is less than 0.3 times the critical energy release rate for crack extension into the fibre.

1. Introduction

In fibre-reinforced metal matrix composites, chemical reaction takes place at the fibre/matrix interface when the composites are exposed at high temperatures. This results in the formation of a reaction layer, which is in most cases brittle and breaks in the early stage of deformation. Once formed, the crack extends into the fibre (Fig. 1a) when the interfacial bonding strength is high, resulting in a strength reduction of the fibres and therefore of the composites [1–4]. One of the methods to avoid the reaction is to coat the fibres. However, if the coating layer is brittle, the fibre strength is reduced, too, because of the same mechanism [5–7].

One of the possible methods to minimize the reduction in fibre strength resulting from the pre-existent crack in the coating layer consists of intentionally weakening the interface [4, 8–12], because if interfacial debonding (Fig. 1b) occurs prior to crack extension into the fibre (Fig. 1a), the fibre strength is not seriously reduced, as has been demonstrated experimentally [8, 9]. On the other hand, in the case where the interfacial bonding strength cannot be reduced or when strong interfacial bonding is required, modification of the coating layer with a properly selected coating material is a possible method to minimize the strength reduction, because the strength of coated fibre is high when the elastic modulus of the coating layer with a pre-existent crack is low [13]. However, for the coating to suppress interfacial reaction, coating materials with low Young's modulus cannot be employed necessarily. Then, as another possible method for minimization of the reduction, double or gradient coating can be considered, because the fact that the use of a low Young's modulus coating material results in small reduction in strength, leads to the speculation that making the Young's modulus of the coating portion adjacent to fibre low by double or gradient coating, will also lead to small reduction.

Until now, the influence of pre-existent crack in such double and gradient coatings on fibre strength has not been clear. Furthermore, the condition for interfacial debonding to occur in such cases is also unknown. The aim of the present work is to know the effects of such coatings on the energy release rates for crack extension into the fibre and for interfacial debonding, and to find the coating condition to minimize the reduction in fibre strength caused by the pre-existent crack in the coating layer.

2. Calculation method

For both crack extension into the fibre and for interfacial debonding, the energy release rate λ is given by

$$\lambda = (P^2/2)\,[\mathrm{d}C(S)/\mathrm{d}S] \quad (1)$$

0022–2461

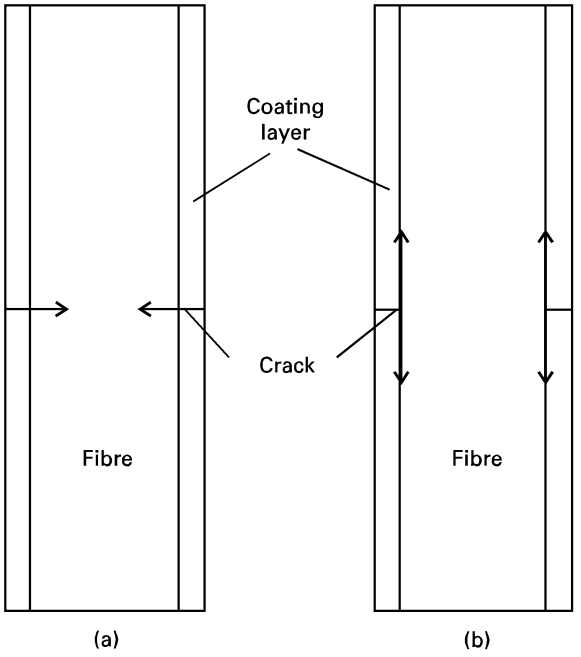

Figure 1 Schematic representation of (a) crack extension into the fibre and (b) interfacial debonding in the coated fibre whose coating layer has a pre-existent crack.

where P is the applied load and $C(S)$ is the compliance for the crack area S. Equation 1 can be modified into the form

$$\lambda = (P^2/2)\left\{\lim_{\Delta S \to 0}[C(S+\Delta S) - C(S)]/(\Delta S)\right\} \quad (2)$$

where ΔS is the increment of cross-sectional area of the crack. When the compliances $C(S)$, $C(S+\Delta S_1)$ and $C(S+\Delta S_2)$, corresponding to the crack areas S, $S+\Delta S_1$ and $S+\Delta S_2$, respectively, are calculated from the applied load and displacement, the energy release rate can be calculated by Equation 2 by extrapolation to $\Delta S = 0$.

In our former works [13–15], a simple calculation method of the energy release rates for crack extension into the fibre and for interfacial debonding, λ_f and λ_i, respectively, for the case of single uniform coating, was presented based on Equation 2 in combination with the shear lag analysis technique. This method allows to calculate the normalized values of λ_f/σ_f^2 and λ_i/σ_f^2, where σ_f is the fibre stress [13–15]. In the present work, this method is extended so as to express the effects of double and gradient coatings and used for calculation.

Fig. 2 shows the schematic representation of the models of the coated fibre for calculation. Cases (a) and (b) correspond to the fibre coated with two layers (layers 1 and 2) and to the one coated with gradient layer. E and G (taken to be $E/2.6$ for all constituents by assuming the Poisson's ratio to be 0.3 in the present work) are Young's and shear moduli, respectively, R_f is the radius of fibre (5 μm), a is the total thickness of the coating layer, and a_1 and a_2 are thicknesses of the layers 1 and 2 in the double-layered coating, respectively (case (a)). The Young's modulus of the fibre was taken to be 400 GPa. For the double coating, the

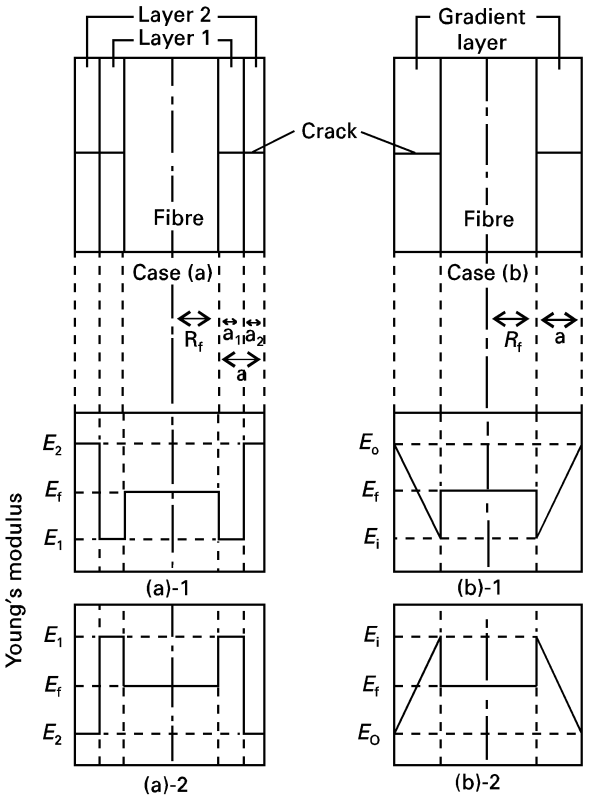

Figure 2 Schematic representation of the models of the double (case (a)) and gradient (case (b)) coatings for calculation. (a) -1 and -2 show the distribution of Young's modulus in the double coating, corresponding to the case where the inner layer 1 and the outer layer 2 have low and high Young's modulus, respectively, and to the case where the layers 1 and 2 have high and low Young's modulus, respectively. (b) -1 and -2 show the distribution of Young's modulus in the gradient coating, corresponding to the case where the inner surface of the coating adjacent to the fibre has low and the outer surface has high Young's modulus, and to the case where the inner and outer surfaces have high and low Young's modulus, respectively.

Young's moduli of the layers 1 and 2 were taken to be 200 and 600 GPa (case (a)-1) and 600 and 200 GPa (case (a)-2), respectively, in order to investigate the influence of the sequence on the energy release rate. For the gradient coating (case (b)), the Young's modulus of the coating layer was assumed to vary linearly in the radial direction, and the Young's moduli of the inner surface of the coating layer adjacent to the fibre (E_i) and to the outer surface (E_o) were taken to be 200 and 600 GPa, respectively, in case (b)-1, and to be 600 and 200 GPa, respectively, in case (b)-2.

3. Results and Discussion

3.1. Influence of pre-existent crack in the double coating on the energy release rates for crack extension into the fibre and for interfacial debonding

3.1.1. Variations of λ_f/σ_f^2 and λ_i/σ_f^2 as a function of total thickness a under a condition of $a_1 = a_2 = a/2$ in double coating

First, the thicknesses of the layers 1 and 2 (a_1 and a_2, respectively) in the double coating (case (a) in Fig. 2)

were taken as half the total thickness a and the variations of λ_f/σ_f^2 and λ_i/σ_f^2 were calculated as a function of a, as shown in Fig. 3a and Fig. 4a, respectively. The results for case (a)-1 ($E_1 = 200$ and $E_2 = 600\,\text{GPa}$) are shown by open circles and those for case (a)-2 ($E_1 = 600$ and $E_2 = 200\,\text{GPa}$) by open triangles. The values of λ_f/σ_f^2 and λ_i/σ_f^2, which would be realized if there were a single layer with a Young's modulus equivalent to the average Young's modulus of the coating (hereafter named as E_{ave}-equivalent single coating for short), were calculated for comparison. The closed circles and triangles show the results corresponding to cases (a)-1 and -2, respectively. From the calculated values of λ_f/σ_f^2 and λ_i/σ_f^2, the strength of fibres determined by crack propagation into the fibre, σ_f^* and the fibre stress at initiation of interfacial

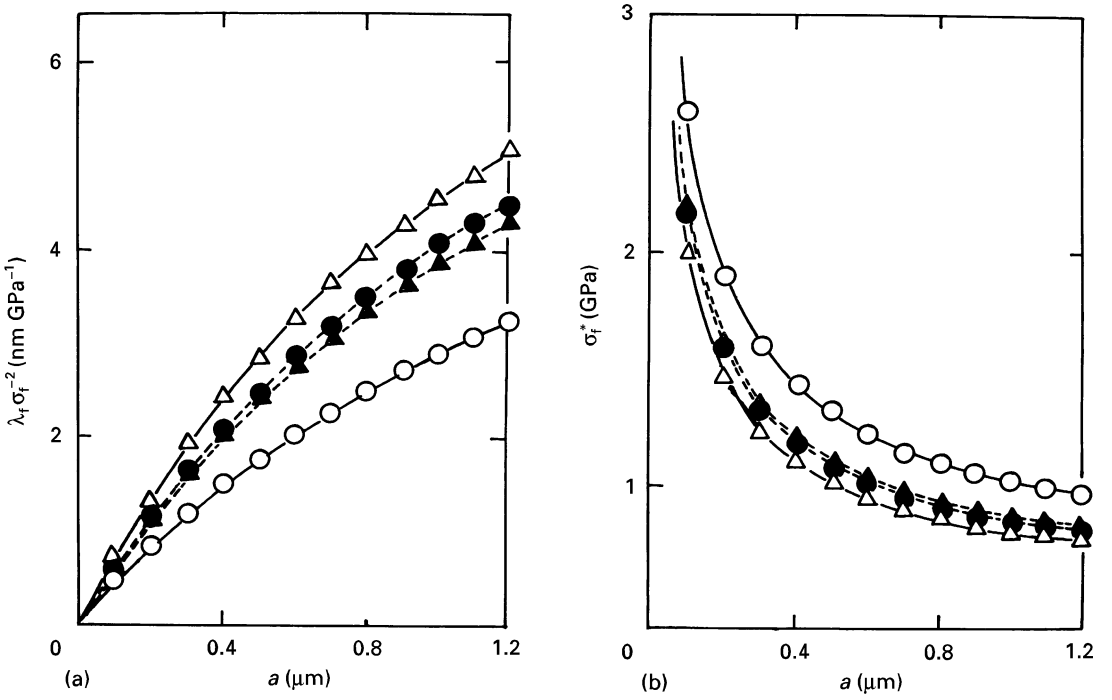

Figure 3 The values of (a) λ_f/σ_f^2 and (b) σ_f^* plotted against a for the cases (a) -1 ((○) $E_1 = 200\,\text{GPa}$; $E_2 = 600\,\text{GPa}$) and -2 ((△) $E_1 = 600\,\text{GPa}$; $E_2 = 200\,\text{GPa}$) under the condition of $a_1 = a_2 = a/2$ in a double coating, together with those for the E_{ave}-equivalent single coating (●) (▲). $\lambda_{f,c} = 3\,\text{Jm}^{-2}$.

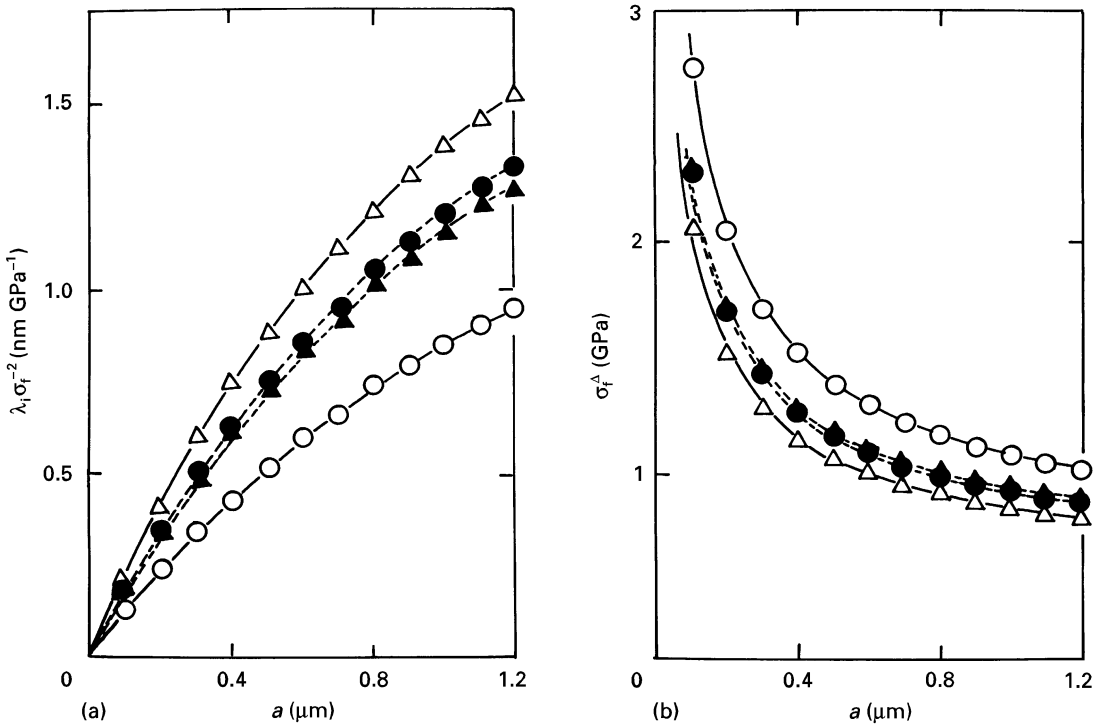

Figure 4 The values of (a) λ_i/σ_f^2 and (b) σ_f^{Δ} plotted against a for the cases (b) -1 and -2 under the condition of $a_1 = a_2 = a/2$ in a double coating, together with those for the E_{ave}-equivalent single coating. $\lambda_{i,c} = 1\,\text{J m}^{-2}$. See Fig. 3 for key.

debonding, σ_f^{Δ}, can be calculated when the critical energy release rates $\lambda_{f,c}$ and $\lambda_{i,c}$ are known. When $\lambda_{f,c}$ and $\lambda_{i,c}$ are taken, for instance, to be 3 and 1 J m^{-2}, respectively, σ_f^* and σ_f^{Δ} can be calculated as shown in Fig. 3b and Fig. 4b, respectively. The following features can be read from Figs 3 and 4.

1. The values of λ_f/σ_f^2 and λ_i/σ_f^2 become high and therefore σ_f^* and σ_f^{Δ} become low when E_1 is high and E_2 is low i.e. when the inner layer 1 has high Young's modulus for any coating thickness a.

2. When the inner layer 1 has high and the outer layer 2 has low Young's modulus, the values of λ_f/σ_f^2 and λ_i/σ_f^2 are higher and therefore the values of σ_f^* and σ_f^{Δ} are lower than those for the E_{ave}-equivalent single coating.

3. When the inner layer 1 has low and outer layer 2 has high Young's modulus, the values of λ_f/σ_f^2 and λ_i/σ_f^2 are lower and the values of σ_f^* and σ_f^{Δ} are higher than those for the E_{ave}-equivalent single coating.

The values of $\sigma_f^*(\sigma_f^{\Delta})$ normalized with respect to the value for the E_{ave}-equivalent single layer coating, $\sigma_{f,o}^*(\sigma_{f,o}^{\Delta})$, can be calculated in the following manner. A schematic representation of the linear relation of $\lambda_f(\lambda_i)$ to σ_f^2 is shown in Fig. 5 in which $\lambda_{f(i)}$ refers to λ_f or λ_i. Using the values of the $\lambda_{f(i)}/\sigma_f^2$ in Figs 3a and 4a, the ratio of $\sigma_f^*(\sigma_f^{\Delta})$ to $\sigma_{f,o}^*(\sigma_{f,o}^{\Delta})$ is given by

$$\sigma_f^*(\sigma_f^{\Delta})/\sigma_{f,o}^*(\sigma_{f,o}^{\Delta}) = \{[\lambda_f(\lambda_i)/\sigma_f^2]/[\lambda_f(\lambda_i)/\sigma_f^2]_{E_{ave}}\}^{1/2} \quad (3)$$

Fig. 6 shows $\sigma_f^*/\sigma_{f,o}^*$ and $\sigma_f^{\Delta}/\sigma_{f,o}^{\Delta}$ calculated in this way against thickness a. The fibre stress for crack extension into the fibre and also the fibre stress for interfacial debonding are about 20% higher than that for E_{ave}-equivalent single coating in case (a)-1, while it is about 8% lower in case (a)-2, for any a. These results mean that: (i) a coating material with low Young's modulus as inner layer can raise the strength of the fibre in the case of strong interfacial bonding and can raise the fibre stress for interfacial debonding in the case of a weak bonding; (ii) the extent of such effects remains nearly constant with increasing thickness of the coating layer; and (iii) the decrease in the stresses for crack extension and for interfacial debonding for case (a)-2 (about 8%) is relatively small in comparison with their increase for case (a)-1 (about 20%).

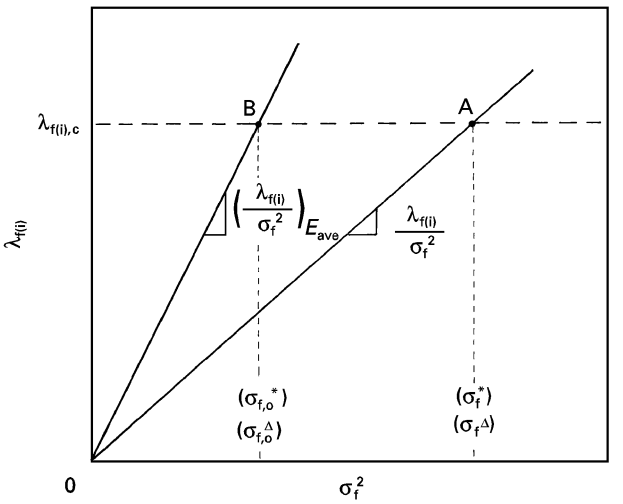

Figure 5 Schematic representation of the relation of λ_f to σ_f^2 and λ_i to σ_f^2. In this figure, $\lambda_{f(i)}$ refers to λ_f or λ_i. When the value of $\lambda_{f(i),c}$ is given, the crack extension (interfacial debonding) occurs at A, corresponding to the stress level of fibre $\sigma_f^*(\sigma_f^{\Delta})$ for double and gradient coatings and it occurs at B for E_{ave}-equivalent single layer coating, corresponding to the stress levels of fibre $\sigma_{f,o}^*(\sigma_{f,o}^{\Delta})$.

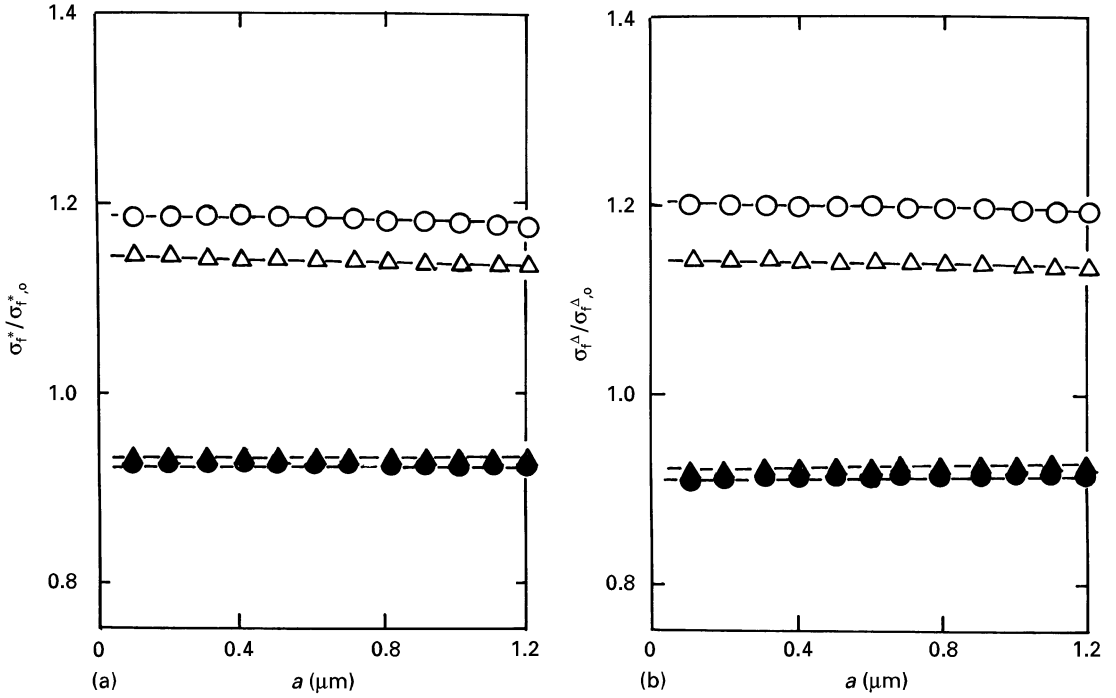

Figure 6 Calculated values of (a) $\sigma_f^*/\sigma_{f,o}^*$ and (b) $\sigma_f^{\Delta}/\sigma_{f,o}^{\Delta}$ plotted against a for the case (a) -1 and -2 under conditions of $a_1 = a_2 = a/2$ in double coating and for the cases (b) -1 and -2 in gradient coating. (○) (a) -1: $E_1 = 200$ GPa, $E_2 = 600$ GPa; (△) (b) -1: $E_i = 200$ GPa, $E_o = 200$ GPa; (●) (a) -2: $E_1 = 600$ GPa, $E_2 = 200$ GPa; (▲) (b) -2: $E_i = 600$ GPa, $E_o = 200$ GPa

3.1.2. Variations of λ_f/σ_f^2 and λ_i/σ_f^2 as a function of thickness of the layer 1 under a condition of the fixed total thickness a = 0.6 μm in double coating

Figs 7a and 8a show the variations of λ_f/σ_f^2 and λ_i/σ_f^2 and Figs 7b and 8b those of σ_f^* and σ_f^Δ as a function of thickness of layer 1, a_1, under the fixed total thickness of the coating $a = 0.6\,\mu m$ for the cases of (a)-1 ($E_1 = 200\,GPa$ and $E_2 = 600\,GPa$ in Fig. 2) and (a)-2 ($E_1 = 600\,GPa$ and $E_2 = 200\,GPa$). Fig. 9 shows the values of $\sigma_f^*/\sigma_{f,o}^*$ and of $\sigma_f^\Delta/\sigma_{f,o}^\Delta$ plotted against a_1 under the same condition. The following features can be read from Figs 7 to 9.

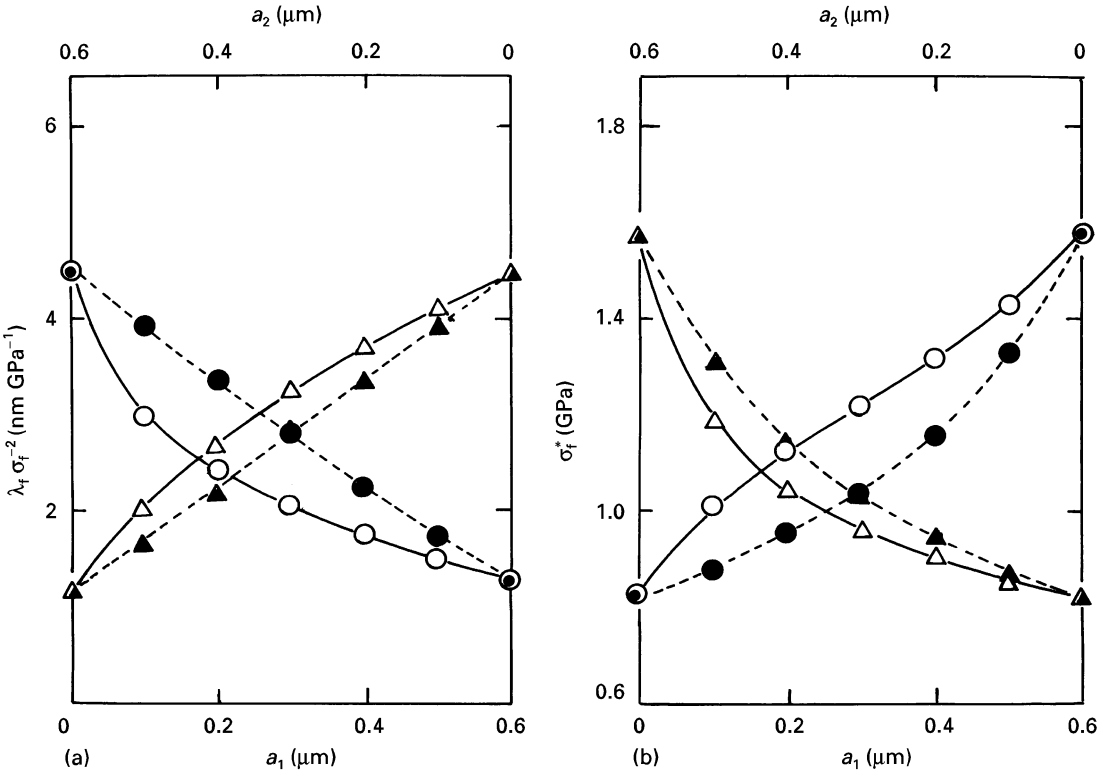

Figure 7 The values of (a) λ_f/σ_f^2 and (b) σ_f^* plotted against a_1 for the cases (a) -1 (circles) and -2 (triangles) under the condition of $a_1 + a_2 = a$ (0.6 μm) in double coating, together with those for the E_{ave}-equivalent single coating (●) (▲). (○) $E_1 = 200\,GPa$, $E_2 = 600\,GPa$; (△) $E_1 = 600\,GPa$, $E_2 = 200\,GPa$. $\lambda_{f,c} = 3\,J\,m^{-2}$.

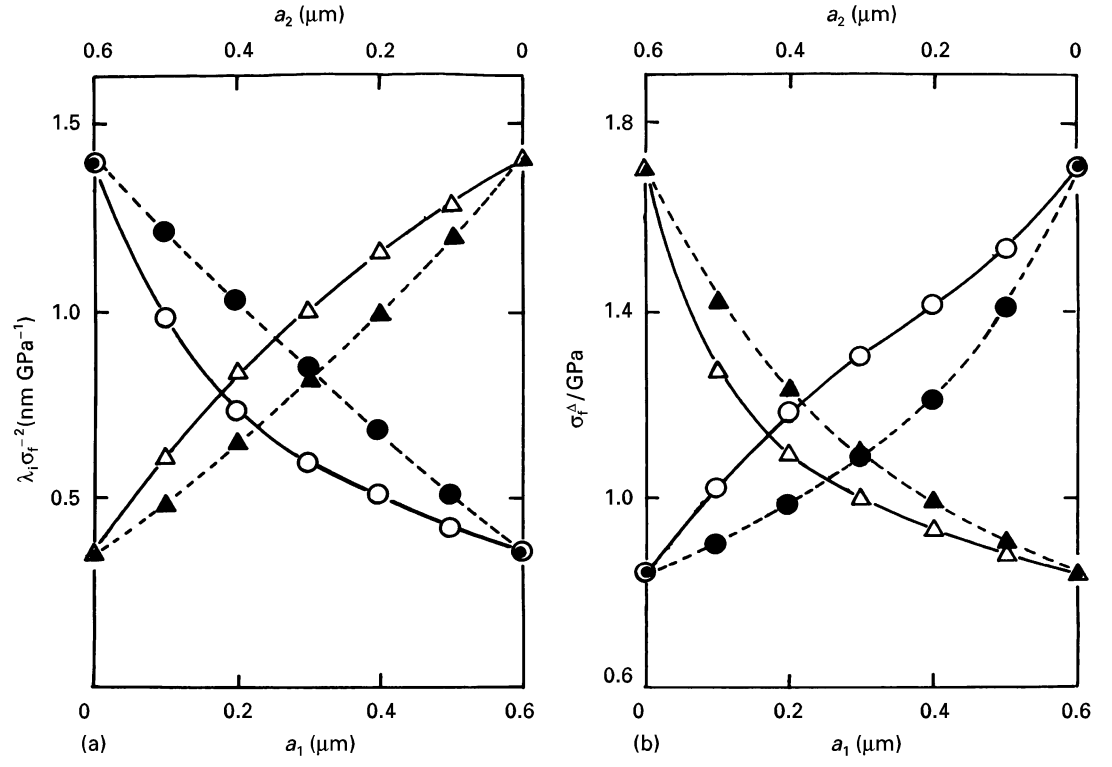

Figure 8 The values of (a) λ_i/σ_f^2 and (b) σ_f^Δ plotted against a_1 for the cases (a) -1 and -2 under the condition of $a_1 + a_2 = a$ (0.6 μm) in double coating, together with those for the E_{ave}-equivalent single coating. $\lambda_{i,c} = 1\,J\,m^{-2}$. See Fig. 7 for key.

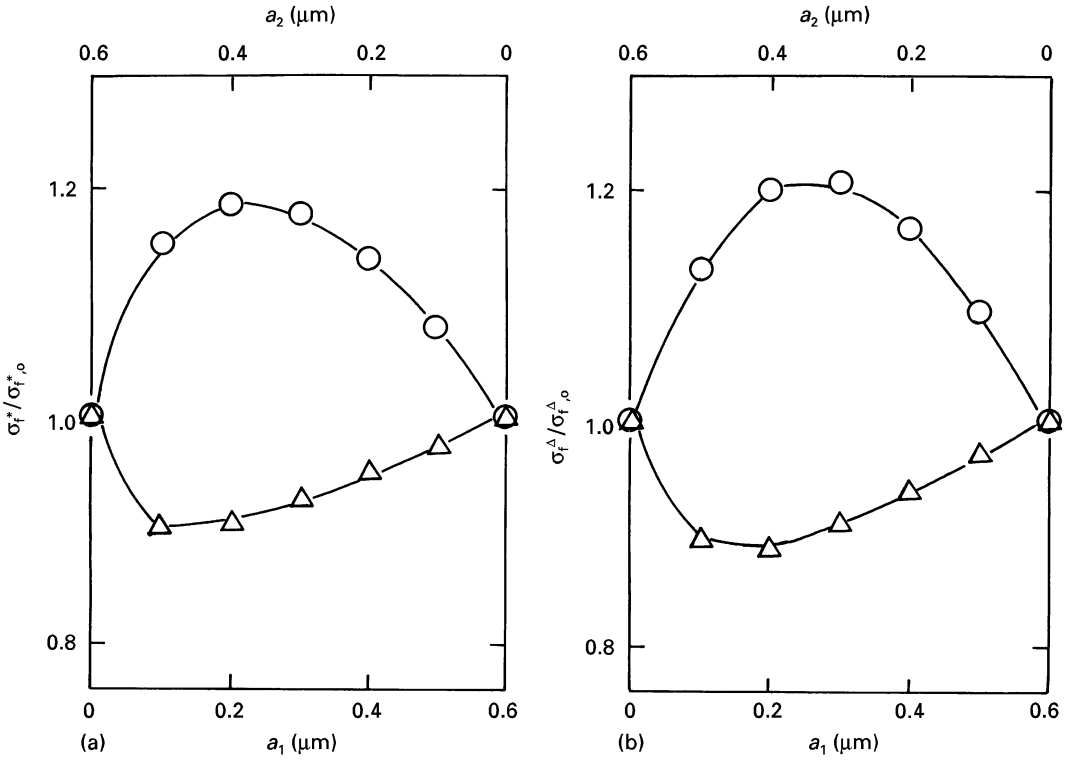

Figure 9 Calculated values of (a) $\sigma_f^*/\sigma_{f,o}^*$ and (b) $\sigma_f^\Delta/\sigma_{f,o}^\Delta$ plotted against a_1 for the case (a) -1 ((○) $E_1 = 200\,\text{GPa}$, $E_2 = 600\,\text{GPa}$) and -2 ((△) $E_1 = 600\,\text{GPa}$, $E_2 = 200\,\text{GPa}$) under a condition of $a_1 + a_2 = a$ (0.6 μm) in double coating.

1. When E_1 is low and E_2 is high ((a)-1), the values of λ_f/σ_f^2 and λ_i/σ_f^2 decrease and therefore σ_f^* and σ_f^Δ increase with increasing a_1, as shown by the open circles (Figs 7 and 8). On the other hand, when E_1 is high and E_2 is low ((a)-2), the former increase and therefore the latter decrease with increasing a_1. Hence, in case (a)-1 as well as in case (a)-2, the larger the proportion of the layer with low Young's modulus, the lower become the energy release rates, and the higher become the stress levels for crack extension and interfacial debonding.

2. In case (a)-1, the values of λ_f/σ_f^2 and λ_i/σ_f^2 (open circles) are lower and therefore the values of σ_f^* and σ_f^Δ are higher than the values for the E_{ave}-equivalent single coating (closed circles). On the other hand, in case (a)-2, the former (open triangles) are higher and the latter are lower than the values for the E_{ave}-coating (closed triangles) (Figs 7 and 8).

3. The values of $\sigma_f^*/\sigma_{f,o}^*$ and $\sigma_f^\Delta/\sigma_{f,o}^\Delta$ for case (a)-1 increase, reach a maximum and then decrease with increasing a_1, while those for case (a)-2 decrease, reach a minimum and then increase with increasing a_1. This result means that the fibre stresses for crack extension into the fibre and for interfacial debonding can be raised in comparison with those for E_{ave}-single layer coating by selecting an appropriate thickness of the layer 1 (0.2–0.3 μm in this example) in case (a)-1.

4. For any a_1 value, the decrease in the stresses for crack extension and interfacial debonding in case (a)-2 is relatively small in comparison with their increase for case (a)-1.

3.2. Influence of pre-existent crack in a gradient coating on the energy release rates for crack extension into the fibre and for interfacial debonding

Fig. 10a and b show the calculated results of λ_f/σ_f^2 and σ_f^*, respectively, for case (b)-1 ($E_i = 200$ and $E_o = 600\,\text{GPa}$) and Fig. 11a and b show those of λ_i/σ_f^2 and σ_f^Δ, respectively, for case (b)-2 ($E_i = 600\,\text{GPa}$ and $E_o = 200\,\text{GPa}$), as a function of a for the gradient coating. The calculated values of $\sigma_f^*/\sigma_{f,o}^*$ and $\sigma_f^\Delta/\sigma_{f,o}^\Delta$ are shown in Fig. 6. The following features can be read from Figs 6, 10 and 11.

1. The calculation results in Figs 10 and 11 for the gradient coating show similar tendency to those for the double-coating shown in Figs 3 and 4 in that energy release rates become high and the stress level for crack extension and debonding become low when the inner portion adjacent to the fibre has a high Young's modulus. The magnitude of the values of E_i and E_o in the gradient coating gives qualitatively similar effects to those of E_1 and E_2 in the double coating.

2. However, quantitatively, slight differences are found in $\sigma_f^*/\sigma_{f,o}^*$ and $\sigma_f^\Delta/\sigma_{f,o}^\Delta$ between the double and gradient coatings, while the values of E_{ave} were nearly the same in the examples in Fig. 6. For a gradient coating, the values of $\sigma_f^*/\sigma_{f,o}^*$ and $\sigma_f^\Delta/\sigma_{f,o}^\Delta$ were about 1.15 and 0.93 for cases (b)-1 and 2, respectively, while for a double coating, those were about 1.20 and 0.92 for cases (a)-1 and 2, respectively. These differences can be attributed to the variation of E with distance in the gradient coating, whereas it remains constant for

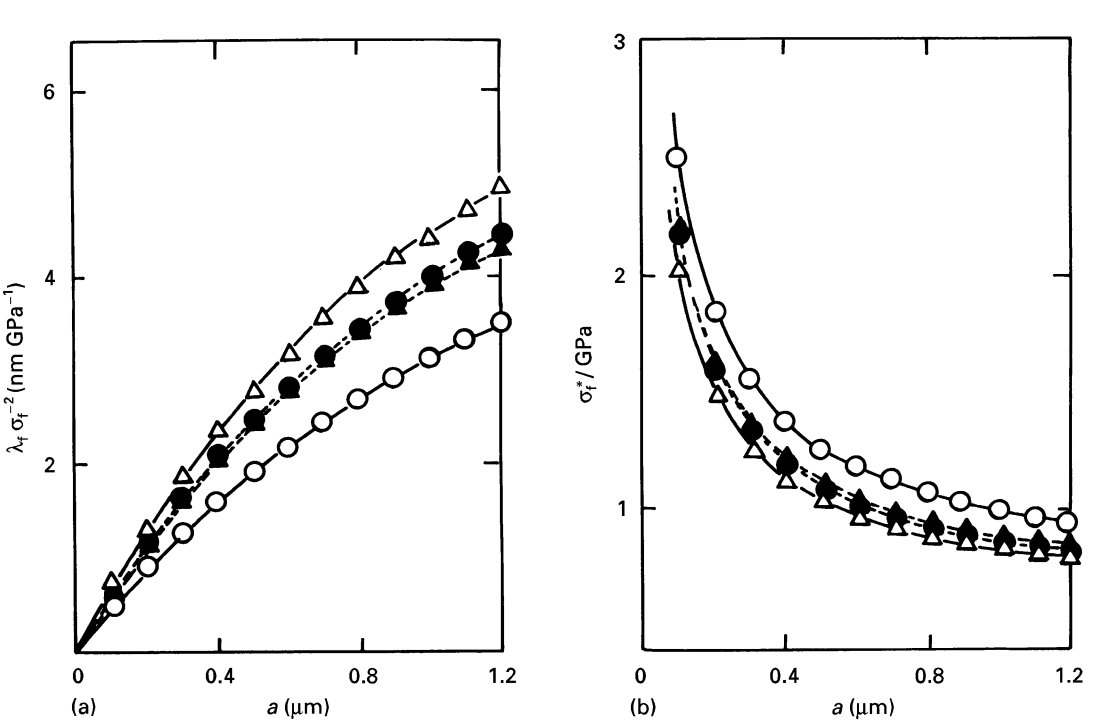

Figure 10 The values of (a) λ_f/σ_f^2 and (b) σ_f^* plotted against a for a gradient coating, together with those for the E_{ave}-equivalent single coating (○) (b) -1: $E_i = 200\,GPa$, $E_o = 600\,GPa$; (●) E_{ave}; (△) (b) -2: $E_i = 200\,GPa$, $E_o = 600\,GPa$; (▲) E_{ave}. $\lambda_{f,c} = 3\,J\,m^{-2}$.

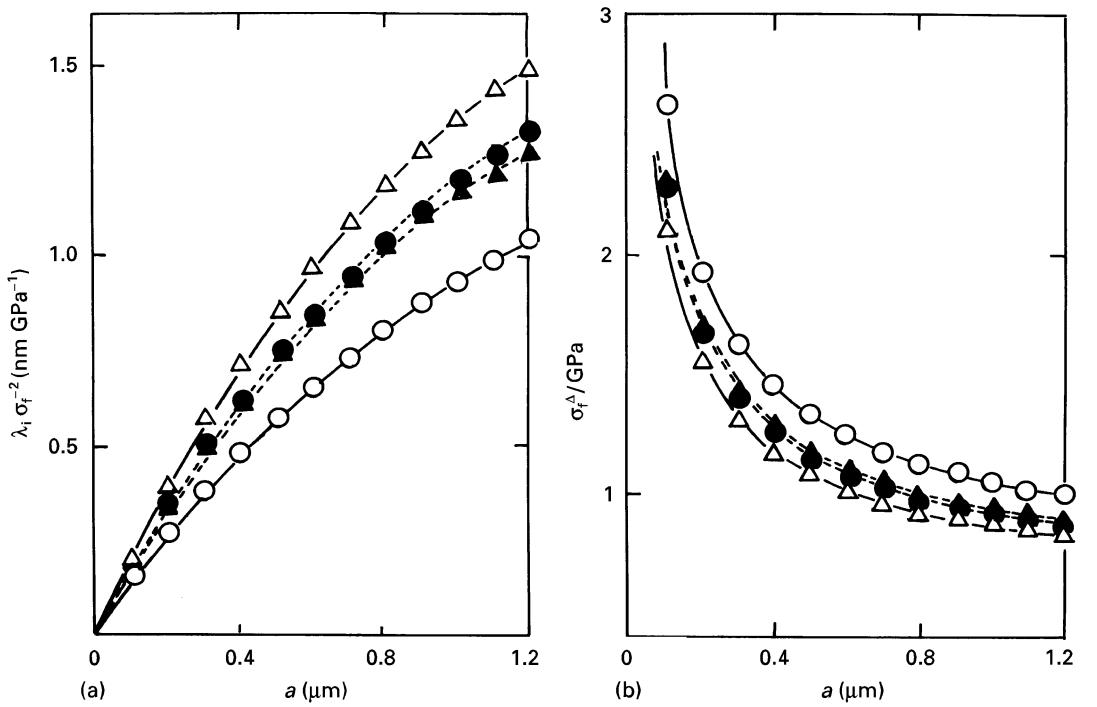

Figure 11 The values of (a) λ_i/σ_f^2 and (b) σ_f^Δ plotted against a in gradient coating, together with the values for the E_{ave}-equivalent single coating. $\lambda_{i,c} = 1\,J\,m^{-2}$. See Fig. 10 for key.

a given location in the double coating. Hence the influence of E_1 for a double coating is more effective than that of E_i for a gradient coating.

3.3. Coating to improve fibre strength

3.3.1. Strong interface

As shown above, when the interfacial bonding strength is high to allow crack propagation into the fibre, a double coating, with an inner layer 1 adjacent to the fibre with low Young's modulus, reduces the decrease in fibre strength caused by crack extension into the fibre if the thickness of the inner layer is appropriate (Figs 3a, 6, 7a). The use of a gradient coating in which Young's modulus decreases from the outer to the inner portion is also useful (Figs 6, 10).

As an example, let us assume the case where the outer surface of the coating is required to have

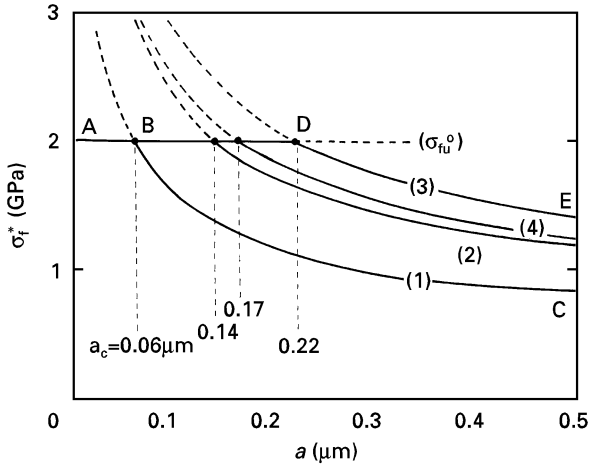

Figure 12 Examples of improvement of fibre strength and allowable thickness a_c for double (curves 2 and 3) and for gradient (curve 4) coatings in comparison with the low fibre strength and small allowable thickness for a single coating with a high Young's modulus (curve 1), in the case of strong interfacial bonding. Curve 1 $E_c = 600\,\text{GPa}$; Curve 2 $E_1 = 200\,\text{GPa}$, $E_2 = 600\,\text{GPa}$, $a_1 = a/3$, $a_2 = 2a/3$, for (a) -1; Curve 3 $E_1 = 200\,\text{GPa}$, $E_2 = 600\,\text{GPa}$, $a_1 = 2a/3$, $a_2 = a/3$, for (a) -1; Curve 4 $E_i = 200\,\text{GPa}$, $E_o = 600\,\text{GPa}$ for (b) -1.

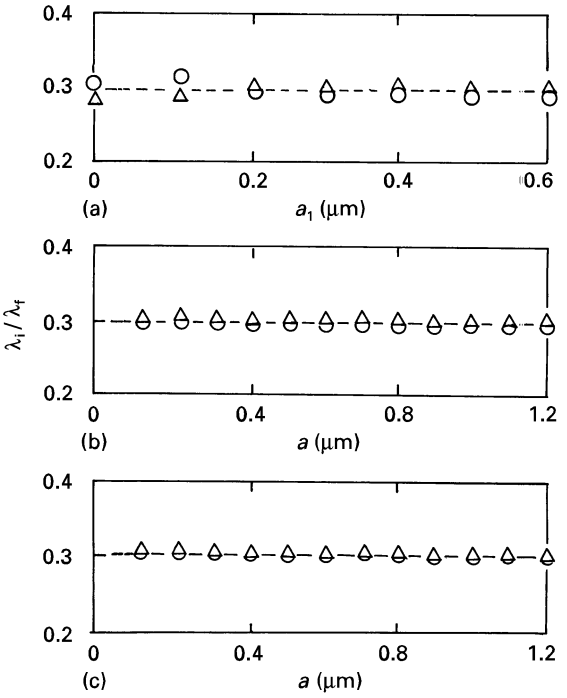

Figure 13 The values of λ_i/λ_f (a) plotted against a_1 for the cases (a) -1 (○) ($E_1 = 200$, $E_2 = 600\,\text{GPa}$) and -2 (△) ($E_1 = 600$, $E_2 = 200\,\text{GPa}$) under a condition of $a_1 + a_2 = a$ (0.6 μm) in the double coating; (b) plotted against a for the cases (a) -1 (○) and -2 (△) under a condition of $a_1 = a_2 = a/2$ in double coating; and (c) plotted against a for the cases of (b) -1 (○) ($E_i = 200$, $E_o = 600\,\text{GPa}$) and -2 (△) ($E_i = 600$ and $E_o = 200\,\text{GPa}$) in the gradient coating.

a Young's modulus 600 GPa for a fibre with $E_f = 400\,\text{GPa}$ and $\lambda_{f,c} = 3\,\text{J m}^{-2}$. In such a case, the use of a single coating layer with a Young's modulus (E_c) of 600 GPa, σ_f^* becomes very low as shown by curve (1) in Fig. 12. If the strength of bare fibre (σ_{fu}^{o}) is assumed to be 2 GPa, the strength of the fibre will be reduced when the thickness of the coating exceeds the critical value a_c which satisfies $\sigma_f^* = \sigma_{fu}^{o}$ since the fibre fails from intrinsic defects for $a < a_c$ [13]. On this point, a_c is regarded as the allowable thickness below which no reduction in fibre strength appears. The value of a_c is 0.06 μm in this case. This means that the thickness of a coating with a Young's modulus of 600 GPa should be controlled to be less than 0.06 μm in order to retain the original fibre strength.

Such a small allowable thickness and low strength of the fibre for $a > a_c$ can be improved by the (a)-1 type double coating with $E_1 = 200$ and $E_2 = 600\,\text{GPa}$ and by (b)-1 type gradient coating with $E_i = 200\,\text{GPa}$ and $E_o = 600\,\text{GPa}$, as shown also in Fig. 12. For case (a)-1, when a_1 and a_2 are set to be $(1/3)a$ and $(2/3)a$, respectively, σ_f^* becomes high as shown by the curve (2) and a_c becomes 0.14 μm. Furthermore, when layer 1 is made thicker ($a_1 = (2/3)a$ and $a_2 = (1/3)a$), σ_f^* becomes much higher, as shown by the curve (3) and a_c becomes 0.22 μm. Also for a gradient coating, σ_f^* becomes high as shown by the curve (4) and a_c becomes 0.17 μm.

In this way, the double and gradient coatings can be utilized to reduce the decrease in fibre strength due to crack extension.

3.3.2. Control of interface to cause debonding prior to crack extension

If interfacial debonding occurs prior to crack extension, the crack tip is blunted and therefore the fibre strength will not be reduced seriously [11–13]. Thus weakening of the interface is an effective way to improve fibre strength [4, 8, 9]. The condition for debonding to occur prior to crack extension is given as follows.

The values of λ_i/σ_f^2 in Figs 4, 8 and 11 were divided by those of λ_f/σ_f^2 in Figs 3, 7 and 10, respectively. The calculated ratio of λ_i/λ_f is shown in Fig. 13. Within the range of the present conditions, the λ_i/λ_f value was almost 0.3. Evans and colleagues [12] have shown that the ratio of λ_i/λ_f in a fibre–brittle matrix composite system is affected by the elastic mismatch given by $(E_f - E_m)/(E_f + E_m)$ with E being the plane strain tensile Young's modulus and the subscripts f and m referring to the fibre and matrix, respectively. As the Young's modulus of the double and gradient coating layers varies with distance from the interface in the present work, our results cannot be compared directly with their results. However, to a first approximation, for $E_f = 400\,\text{GPa}$ and E_m (regarded as Young's modulus of the coating layer in the present system) = 600 to 200 GPa, the elastic mismatches are -0.2 to 0.33, respectively. For these values, the values of λ_i/λ_f are read to be 0.25 to 0.32 from the result of Evans and co-workers [12]. The present result of $\lambda_i/\lambda_f \approx 0.3$ is similar to their result, indicating that the value of λ_i/λ_f of the double and gradient coatings is not so much different from that of a single coating, to a first approximation. These results suggest that the condition for debonding to occur prior to crack extension into fibre is approximately given by $\lambda_{i,o} < 0.3\lambda_{f,c}$ for single, double and gradient coatings.

4. Conclusions

1. The energy release rates for crack extension into the fibre and for interfacial debonding become low and therefore the stresses for crack extension and debonding become high when the inner portion adjacent to the fibre has a low Young's modulus in double and gradient coatings, while they become high and therefore the stresses become low when the inner portion has high Young's modulus.

2. The ratio of the energy release rate for interfacial debonding to that for crack extension is approximately 0.3 within the present condition for $E_f = 400\,GPa$ and $E_1(E_i) = 200$ to $600\,GPa$ and $E_2(E_o) = 600$ to $200\,GPa$ in both double and gradient coatings.

3. Even if the interfacial bonding strength is high, the reduction in fibre strength due to crack extension into fibre can be made smaller by reducing the Young's modulus of the inner coating portion in the double and gradient coatings.

4. The fibre strength can be raised by weakening the interface as to have the critical energy release rate for debonding less than 0.3 times the critical energy release rate for crack extension into the fibre.

References

1. A. G. METCALFE and M. J. KLEIN, "Interface in metal matrix composites" (Academic Press, New York, 1974) p. 125.
2. J. A. DICARLO, "Proceedings Mechanical behaviour of metal/matrix composites" (AIME, Pennsylvania, 1983) p. 1.
3. S. OCHIAI, "Mechanical properties of metallic composites" (Marcel Dekker Inc., New York, 1993) p. 473.
4. S. OCHIAI and M. HOJO, *Composite Interfaces* **2** (1994) 365.
5. K. HONJO and A. SHINDO, *J. Mater. Sci.* **21** (1986) 1879.
6. D. D. HIMBEAULT, R. A. VARIN and K. PIEKARSKI, *ibid.* **24** (1989) 2746.
7. *Idem., Metall Trans. A* **20A** (1988) 165.
8. S. OCHIAI, S. URAKAWA, K. AMEYAMA and Y. MURAKAMI, *ibid.* **11A** (1980) 525.
9. Y. MURAKAMI, K. NAKAO, A. SHINDO, K. HONJO and S. OCHIAI, in Proceedings of the International Symposium on Composite Materials and Structures, Beijing, China, June (1986) p. 1045.
10. A. G. EVANS, *Mater. Sci. Engng* **A107** (1989) 227.
11. P. G. CHARALAMBIDES and A. G. EVANS, *J. Amer. Ceram. Soc.* **72** (1989) 746.
12. A. G. EVANS, M. Y. HE and J. W. HUTCHINSON, *ibid.* **72** (1989) 2300.
13. S. OCHIAI, K. OSAMURA and K. HONJO, *Mater. Sci. Engng* **A154** (1992) 149.
14. S. OCHIAI and M. HOJO, *Mater. Trans., JIM* **34** (1993) 563.
15. S. OCHIAI and K. OSAMURA, *Z. Metallkde* **84** (1993) 690.

Received 23 September 1996
and accepted 5 August 1997